



Proceeding Paper

Estimation of Land Surface Temperature from the Joint Polar-Orbiting Satellite System Missions: JPSS-1/NOAA-20 and JPSS-2/NOAA-21 [†]

Fatima Zahrae Rhziel , Mohammed Lahraoua * and Naoufal Raissouni

Systems and Telecommunications Research Unit, National School for Applied Sciences of Tetouan, University Abdelmalek Essaadi, Remote Sensing, Tetouan 93000, Morocco;

fatimazahrae.rhziel@etu.uae.ac.ma (F.Z.R.); naoufal.raissouni.ensa@gmail.com (N.R.)

* Correspondence: m_lahraoua@yahoo.fr

[†] Presented at the 5th International Electronic Conference on Remote Sensing, 7–21 November 2023;

Available online: <https://ecrs2023.sciforum.net/>.

Abstract: The accurate estimation of land surface temperature (LST) is a vital parameter in various fields, such as hydrology, meteorology, and surface energy balance analysis. This study focuses on the estimation of LST using data acquired from Joint Polar-Orbiting Satellite System (JPSS) satellites, specifically JPSS-1/NOAA-20 and JPSS-2/NOAA-21. The methodology for this research centers on the utilization of the split-window algorithm, a well-established and recognized technique renowned for its proficiency in extracting accurate land surface temperature (LST) values from remotely sensed data. This algorithm leverages the differential behavior of thermal infrared (TIR) radiance measured in two adjacent spectral channels to estimate LST, effectively mitigating the influence of atmospheric distortions on the acquired measurements. To establish the accuracy of the proposed approach, the coefficients of the split-window algorithm were determined using linear regression analysis, utilizing a dataset generated via extensive radiative transfer modeling. The calculated LST values were subsequently compared with LST products provided by the National Oceanic and Atmospheric Administration (NOAA). The evaluation process encompassed the computation of root mean square error (RMSE) values, offering insights into the performance of the algorithm for both JPSS-1/NOAA-20 and JPSS-2/NOAA-21 missions. LST retrieval validation with standard atmospheric simulation indicates that the JPSS-1/NOAA-20 and The JPSS-1/NOAA-21 algorithms have demonstrated an accuracy of 1.4 K in retrieval of LST with different errors. The obtained results demonstrate the potential of the split-window algorithm to effectively estimate LST from JPSS satellite data. The RMSE values, 2.05 and 1.71 for JPSS-1/NOAA-20 and JPSS-2/NOAA-21, respectively, highlight the algorithm's capability to provide accurate LST estimates for different mission datasets. This research contributes to enhancing our understanding of land surface temperature dynamics using remote sensing technology and showcases the valuable insights that can be gained from JPSS missions in monitoring and studying Earth's surface processes.

Keywords: land surface temperature; split-window algorithm; JPSS-1/NOAA-20; JPSS-2/NOAA-21



Citation: Rhziel, F.Z.; Lahraoua, M.; Raissouni, N. Estimation of Land Surface Temperature from the Joint Polar-Orbiting Satellite System Missions: JPSS-1/NOAA-20 and JPSS-2/NOAA-21. *Environ. Sci. Proc.* **2024**, *29*, 38. <https://doi.org/10.3390/ECRS2023-15847>

Academic Editor: Riccardo Buccolieri

Published: 6 November 2023



Copyright: © 2023 by the authors. Licensee MDPI, Basel, Switzerland. This article is an open access article distributed under the terms and conditions of the Creative Commons Attribution (CC BY) license (<https://creativecommons.org/licenses/by/4.0/>).

1. Introduction

Land Surface Temperature (LST) is a fundamental element within the realm of land surface dynamics, capturing the intricate interplay between the Earth's surface and the surrounding atmosphere, as well as the exchange of energy between them [1–4]. LST serves a critical role in a wide range of applications, including the modeling of evapotranspiration [5,6], the evaluation of soil moisture levels [7–9], and the exploration of climatic, hydrological, and ecological patterns [10–17]. LST is obtained from satellite data through a process that involves correcting for atmospheric influences, addressing the absorption and emission of atmospheric surface emissivity and water vapor [18–33]. LST retrieval

relies on the application of the split-window technique. The development of Split-Window (SW) algorithms is rooted in variations associated with atmospheric effects and surface emissivity [19,20,34–36].

Surface emissivity corresponds to the radiative flux of thermal radiation emitted by a surface element. It is crucial for determining the thermal radiation from the Earth’s surface and is a fundamental parameter that influences the accuracy and efficiency of LST retrieval.

Hence, fluctuations in atmospheric transmittance are closely linked to the dynamics of water vapor content within the atmospheric profile for thermal channels [28]. In this paper, we compared operativity, performance, and effectivity of Joint Polar-Orbiting Satellites JPSS-1/NOAA-20 and JPSS-2/NOAA-21’s algorithms for retrieving LST NOAA data [37].

2. The Radiative Transfer Equation Role in Land Surface Temperature Estimation

The radiative transfer equation represents a fundamental principle, used in various fields of science and engineering, including astrophysics, atmospheric science, remote sensing, and heat transfer. It describes the transport of radiant energy such as electromagnetic radiation through a medium.

The equation is particularly useful for understanding how energy is absorbed, scattered, and transmitted as it interacts with particles or substances within a medium.

In clear-sky conditions, the top-of-atmosphere radiance recorded with a space-borne sensor $L_{\text{sensor},\lambda}$ comprises contributions from the surface emission. The atmospheric, upwelling and downwelling radiance $L_{\text{atm},\lambda}^{\uparrow}$ and $L_{\text{atm},\lambda}^{\downarrow}$ is reflected by the ground surface and attenuated by the atmosphere (Equation (1)). The retrieval algorithms depend on one or more top-of-atmosphere spectral measurements to account for atmospheric effects and estimate LST.

$$L_{\text{sensor},\lambda} = \left[\varepsilon_{\lambda} B(T_s) + (1 - \varepsilon_{\lambda}) L_{\text{atm},\lambda}^{\downarrow} \right] \tau_{\lambda} + L_{\text{atm},\lambda}^{\uparrow} \tag{1}$$

where $B(T_s)$ refers to blackbody radiance as defined by Planck’s law, T_s represents the land surface temperature, and ε_{λ} stands for the land surface emissivity.

The Visible Infrared Imaging Radiometer Suite (VIIRS) LST is established through comparisons with ground-based measurements and LST products from other instruments, particularly the NOAA series of LST products.

3. LST Inversion Techniques

Obtaining atmospheric parameters from in situ radiosoundings and using radiative transfer are common approaches in remote sensing and atmospheric science. These atmospheric parameters are essential for correcting remote sensing data, particularly for estimating land surface temperature accurately.

The atmospheric parameters are acquired through in situ radiosoundings and the utilization of radiative transfer codes, such as MODTRAN [38]. Equation (1) has the potential to calculate T_s by inverting Planck’s law. The inversion of Equation (1) can be achieved by correcting for atmospheric and emissivity effects.

Therefore, Inverting Planck’s law involves

$$T_s = \frac{C_1}{\lambda \ln \left(\frac{C_2}{\frac{\lambda^5 (B(T_s) + L_{\text{sensor},\lambda} - (1 - \varepsilon_{\lambda}) L_{\text{atm},\lambda}^{\downarrow})}{\tau_{\lambda} \varepsilon_{\lambda}}} + 1 \right)} \tag{2}$$

where λ is the effective band wavelength and Planck’s law constants: $C_1 = 14,387.7 \mu\text{m} \cdot \text{K}$ and $C_2 = 1.19104 \times 10^8 \text{ W} \cdot \mu\text{m}^4 \cdot \text{m}^{-2} \cdot \text{sr}^{-1}$.

The atmospheric parameters were derived from the Operational Vertical Sounder (TOVS) Thermodynamic Initial Guess Retrieval (TIGR3) database [39] and simulated using the MODTRAN model.

Split-Window Algorithm for Land Surface Temperature Estimation

The SW algorithm is a widely used method for estimating land surface temperature (LST) based on remote sensing data in the thermal infrared region and depends on the differential absorption characteristics of two thermal infrared channels.

The SW algorithm applies quadratic combination of brightness temperatures to calculate LST [39]. It estimates LST by exploiting the distinct atmospheric absorptions in two adjacent thermal infrared spectral regions, assuming known emissivity. SW algorithm coefficients are sensitive, affected by changing total column water vapor (WVC) and various viewing angles [19,34,36].

The SW algorithm has been widely used by researchers to retrieve both sea surface temperature (SST) and land surface temperature (LST) from remote sensing data. In this paper, the two-channel algorithm proposed by [36] has been used, which takes into account the emissivity and water vapor effects.

The formula of the SW algorithm is as follows:

$$T_s = T_i + c_1(T_i - T_j) + c_2(T_i - T_j)^2 + c_0 + (c_3 + c_4W)(1 - \epsilon) + (c_5 + c_6W)\Delta\epsilon \quad (3)$$

In this formula, T_s represents the surface temperature (in Kelvin), T_i and T_j are the brightness temperatures from different thermal channels (in Kelvin), ϵ is the mean effective emissivity, $\Delta\epsilon$ is the emissivity difference, w is the total atmospheric water vapor (in grams per square centimeter), and c_0 to c_6 denote the SW coefficients.

4. MODTRAN for Simulating Atmospheric Parameters

The atmospheric parameters' determination is completed through simulations that account for local atmospheric conditions, particularly water vapor content. These simulations establish the relationship between atmospheric transmittance and water vapor content and are conducted using atmospheric modeling software like MODTRAN (MODerate spectral resolution atmospheric TRANsmission). MODTRAN is widely employed in the fields of remote sensing and atmospheric research to calculate anticipated brightness temperatures for specific thermal channels on JPSS-1/NOAA-20 and JPSS-2/NOAA-21 satellites. MODTRAN serves as a well-established tool for modeling the radiative transfer of electromagnetic radiation through Earth's atmosphere.

Temperature profiles were meticulously derived from radiosoundings, originating from the Television InfraRed Observation Satellite (TIROS) Operational Vertical Sounder (TOVS) Thermodynamic Initial Guess Retrieval (TIGR3) database [39]. These calculations spanned a wide spectrum of temperature gradients.

Furthermore, the calculations encompassed various viewing angles, a comprehensive range of atmospheric-water-vapor values, and 100 distinct emissivity values obtained from spectral responses of diverse surface types available in the Advanced Spaceborne Thermal Emission Reflection Radiometer (ASTER) spectral library [40].

The MODTRAN outputs provide essential atmospheric parameter values: atmospheric transmittances, atmospheric upwelling and downwelling radiances. These values are acquired through mathematical convolution employing two filter functions that correspond to the thermal infrared channels of the JPSS-1/NOAA-20 and JPSS-2/NOAA-21 satellites.

5. Numerical Coefficients and Sensitivity Analysis

The SW algorithm coefficients refer to the parameters used in the SW algorithm for estimating LST from TIR remote sensing satellite. These coefficients are crucial for the algorithm, as they are used in the mathematical equations to convert the observed radiance values into LST values.

The coefficients in Equation (1) were calculated through the minimization of simulations from a constructed database for the JPSS-1/NOAA-20 and JPSS-2/NOAA-21 satellites.

To assess the influence of individual error sources on the SW algorithm, a sensitivity analysis was conducted. This analysis aimed to evaluate the algorithm’s performance across a range of meteorological conditions and land cover types:

$$\delta_{\text{Total}}(T_s) = \sqrt{\delta_{\text{alg}}^2 + \delta_{\text{NE}\Delta E}^2 + \delta_{\epsilon}^2 + \delta_W^2} \tag{4}$$

The total error in LST is calculated from elementary errors: the algorithm standard deviation, the impact of uncertainties in at-sensor temperatures, land surface emissivity, and atmospheric water vapor.

6. Analysis of Split-Window Algorithm Coefficients and Sensitivity Results

Sensitivity analysis, which includes factors such as land surface emissivity, channel noise, water vapor, is a crucial element in the assessment of the performance and precision of LST retrieval algorithms.

The SW coefficients present in Table 1 were obtained from regressions methods for the JPSS-1/NOAA-20 and JPSS-2/NOAA-21 satellites.

Table 1. JPSS-1/NOAA-20 and JPSS-2/NOAA-21 satellites: Split-Window Algorithm coefficients.

Satellites	C ₀	C ₁	C ₂	C ₃	C ₄	C ₅	C ₆
NOAA-11	0.021	1.878	0.268	57.2	0.07	−132	10.31
NOAA-12	0.030	1.623	0.306	57.1	−0.08	−135	12.12
JPSS-1/NOAA-20	−0.16	1.330	0.230	58.1	−0.57	−112	8.84
JPSS-2/NOAA-21	0.079	1.297	0.216	58.6	−0.62	−99	5.88

Table 2 illustrates the impact of minimization errors for JPSS-1/NOAA-20 and JPSS-2/NOAA-21 in Kelvin (K). The respective values are 1.09 K and 1.07 K, with corresponding correlation coefficients (R) of 0.91 and 0.93. Additionally, there are noise-induced errors of 0.23 K and 0.22 K, as well as errors attributed to atmospheric-water-vapor content uncertainty, which amount to 0.04 K and 0.02 K.

Table 2. The sensitivity analysis of impacting factors for JPSS-1/NOAA-20 and JPSS-2/NOAA-21.

Satellite	R	δ_{alg} (K)	$\delta_{\text{NE}\Delta T}$ (K)	δ_{ϵ} (1%)	δ_{ϵ} (0.5%)	δ_W (K)	$\delta_{\text{Total}}(T_s)$ (1%)	$\delta_{\text{Total}}(T_s)$ (0.5%)
NOAA-11	0.96	1.04	0.29	1.57	0.79	0.03	1.91	1.34
NOAA-12	0.94	1.06	0.28	1.56	0.78	0.06	1.91	1.35
JPSS-1/NOAA-20	0.91	1.09	0.23	1.35	0.67	0.04	1.75	1.30
JPSS-2/NOAA-21	0.93	1.07	0.22	1.26	0.63	0.02	1.67	1.26

When accounting for a 1% uncertainty in surface emissivity, the LST total error is 1.75 K and 1.67 K for JPSS-1/NOAA-20 and JPSS-2/NOAA-21, respectively. If the surface emissivity uncertainty is reduced to 0.05%, the total error becomes 1.30 K and 1.26 K for the two respective satellites.

7. Split-Window Algorithm Validation

Validation methods are essential for assessing whether land surface temperature (LST) data conform to the specified standards or accuracy requirements. Ground-based validation is a common approach that involves comparing remote sensing-derived LST values with measurements collected on the ground. This method has been widely employed to validate LST products.

Sensitivity analysis serves to evaluate the impact of potential errors in the SW algorithm retrieval. Additionally, validation is imperative to discover the algorithm’s alignment with real-world LST values. In this study, two distinct validation methods were employed: standard atmospheric simulations and ground truth datasets supplied by [41].

Two homogeneous surface sites located in Australia were used for LST validation; their geolocation and surface type are presented in Table 3. The mean emissivity was given by Prata in [41] of 0.98 for both sites.

Table 3. Geolocation and surface type of the two sites.

Site Location	Altitude	Longitude	Surface Type
Walpeup, northwest of Melbourne	35°12' S	142°36' E	Cropland
Hay, New South Wales	23°24' S	145°18' E	Vegetation/soil mixture

The AD592 solid-state temperature transducers were employed to perform in situ temperature measurements at both sites. Detailed information about the functioning of these devices is provided by [42].

Table 4 presents the validation for NOAA algorithm series in comparison to the ground truth dataset. The last column of the table provides the RMSE values for the algorithms when applied to the total data acquired at the sites, Hay and Walpeup.

Table 4. SW algorithms' validation using ground truth datasets.

Sensor	Mean Differences (Bias) (K)	Standard Deviation of Differences (K)	Root Mean Square Error (K)
NOAA-11	0.74	1.37	1.87
NOAA-12	0.77	1.33	1.77
JPSS-1/NOAA-20	1.10	1.43	2.05
JPSS-1/NOAA-21	0.97	1.31	1.71

The results demonstrate the successful derivation of an LST NOAA series using these algorithms, characterized by mean difference values of 1.10 K for JPSS-1/NOAA-20 and 0.97 K for JPSS-2/NOAA-21, respectively. Additionally, these algorithms yield LST data with a standard deviation of approximately 2.05 K for JPSS-1/NOAA-20 and less than 1.71 K for JPSS-2/NOAA-21 at both the Hay and Walpeup sites.

The analysis results demonstrate the SW capability to generate LST RMSE values ranging between 1.61 K and 1.96 K for the Hay and Walpeup locations (NOAA11 dataset) and between 1.71 K and 2.05 K for the Hay and Walpeup locations (NOAA12 dataset). Furthermore, Figure 1 shows good matching between the NOAA-20 and NOAA-21 retrieved LSTs and the measured ones, with a correlation coefficient of 0.98.

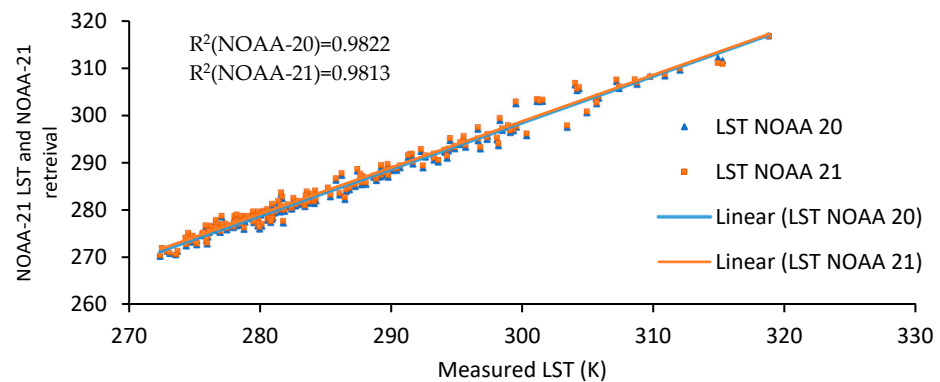


Figure 1. Validation of NOAA-21 and NOAA-20 split-window algorithm using the ground truth dataset of [41].

The satisfactory performance of the JPSS algorithms during the validation process, utilizing datasets, underscores the algorithm's capability to deliver precise land surface

temperature (LST) estimations under well-defined atmospheric transmittances, ground emissivity, and atmospheric-water-vapor conditions. The accuracy of algorithms, establishes this as a favorable choice for applications involving the retrieval of LST from VIIRS satellites data.

8. Conclusions

The JPSS-1/NOAA-20 and The JPSS-1/NOAA-21 algorithms are used to retrieve LST in this study. The algorithms' coefficients were obtained from the atmospheric profiles' dataset simulation. The ground data was used to evaluate the algorithms.

The validation and comparison using the ground truth datasets from two Australian sites, confirm JPSS algorithm performances. Basing the RMSE of the retrieved LSTs on the measured data, the algorithm is very powerful in its LST calculation. The accuracy of LST retrieval is compared to that of NOAA-11 and 12. The algorithms have a higher accuracy with the ground truth dataset for NOAA-11 and 12 with precise in situ atmospheric-water-vapor contents. The sensitivity analysis validation, shows accuracy of 1.4 K in LST retrieval for the JPSS-1/NOAA-20 and JPSS-1/NOAA-21 algorithms. The accuracy of these algorithms is about 1.71 K and 2.05 for the ground truth dataset.

Author Contributions: Conceptualization, F.Z.R.; methodology, all authors; formal analysis, M.L.; investigation, all authors; original draft preparation, F.Z.R.; writing review and editing, all authors; visualization, M.L.; supervision, N.R. All authors have read and agreed to the published version of the manuscript.

Funding: This research received no external funding.

Institutional Review Board Statement: Not applicable.

Informed Consent Statement: Not applicable.

Data Availability Statement: The VIIRS channels JPSS-2/NOAA-21 and JPSS-1/NOAA-20 filters are obtained from the websites: https://ncc.nesdis.noaa.gov/NOAA-20/J1VIIRS_NOAA20_SpectralResponseFunctions.php, https://ncc.nesdis.noaa.gov/NOAA-21/J2VIIRS_SpectralResponseFunction.s.php, while validation data are acquired from The Global Change Unit (GCU) of the University of Valencia in Spain.

Conflicts of Interest: The authors declare no conflict of interest.

References

1. Anderson, M.; Norman, J.; Kustas, W.; Houborg, R.; Starks, P.; Agam, N. A thermal-based remote sensing technique for routine mapping of land-surface carbon, water and energy fluxes from field to regional scales. *Remote Sens. Environ.* **2008**, *112*, 4227–4241. [[CrossRef](#)]
2. Mannstein, H. Surface Energy Budget, Surface Temperature and Thermal Inertia. In *Remote Sensing Applications in Meteorology and Climatology*; Vaughan, R.A., Ed.; Springer: Dordrecht, The Netherlands, 1987; pp. 391–410.
3. Sellers, P.; Hall, F.; Asrar, G.; Strebel, D.; Murphy, R. The first ISLSCP field experiment (FIFE). *Bull. Am. Meteorol. Soc.* **1988**, *69*, 22–27. [[CrossRef](#)]
4. Diak, G.R.; Whipple, M.S. Improvements to models and methods for evaluating the land-surface energy balance and effective roughness using radiosonde reports and satellite-measured skin temperature data. *Agric. Forest Meteorol.* **1993**, *63*, 189–218. [[CrossRef](#)]
5. Brunsell, N.A.; Gillies, R.R. Length scale analysis of surface energy fluxes derived from remote sensing. *J. Hydrometeorol.* **2003**, *4*, 1212–1219. [[CrossRef](#)]
6. Olioso, A.; Chauki, H.; Couraul, D.; Wigneron, J.P. Estimation of evapotranspiration and photosynthesis by assimilation of remote sensing data into SVAT models. *Remote Sens. Environ.* **1999**, *68*, 341–356. [[CrossRef](#)]
7. Chehbouni, A.; Lo Seen, D.; Joku, E.G.; Onteny, B.A. Examination of the difference between radiative and aerodynamic surface temperatures over sparsely vegetated surfaces. *Remote Sens. Environ.* **1996**, *58*, 177–186. [[CrossRef](#)]
8. Schmugge, T.J. Remote sensing of surface soil moisture. *J. Appl. Meteorol. Climatol.* **1978**, *17*, 1557–1978. [[CrossRef](#)]
9. Price, J.C. The potential of Remotely Sensed Thermal Infrared data to Infer Surface Soil Moisture and Evaporation. *Water Resour.* **1990**, *16*, 787–795. [[CrossRef](#)]
10. Santanello, J.; Peters-Lidard, C.D.; Garcia, M.E.; Mocko, D.M.; Tischler, M.A.; Moran, M.S.; Thoma, D.P. Using remotely-sensed estimates of soil moisture to infer soil texture and hydraulic properties across a semi-arid watershed. *Remote Sens. Environ.* **2007**, *110*, 79–97. [[CrossRef](#)]

11. Schmugge, T.J.; André, J.-C. *Land Surface Evaporation: Measurement and Parameterization*; Springer: New York, NY, USA, 1991.
12. Arnfield, A.J. Two decades of urban climate research: A review of turbulence, exchanges of energy and water, and the urban heat island. *Int. J. Climatol.* **2003**, *23*, 1–26. [[CrossRef](#)]
13. Hansen, J.; Ruedy, R.; Sato, M.; Lo, K. Global surface temperature change. *Rev. Geophys.* **2010**, *48*, RG4004. [[CrossRef](#)]
14. Parkinson, C.L.; Greenstone, R.; Closs, J. *EOS Data Products Handbook*; NASA Goddard Space Flight Center: Greenbelt, MD, USA, 2000; Volume 2.
15. Oyoshi, K.; Akatsuka, S.; Takeuchi, W.; Sobue, S. Hourly LST Monitoring with Japanese Geostationary Satellite MTSAT-1R over the Asia-Pacific Region. *Asian J. Geoinform.* **2014**, *14*, 1–13.
16. Running, S.W.; Justice, C.O.; Salomonson, V.; Hall, D.; Barker, J.; Kaufman, Y.; Strahler, A.; Huete, A.; Muller, J.-P.; Vanderbilt, V.; et al. Terrestrial remote sensing science and algorithms planned for EOS/MODIS. *Int. J. Remote Sens.* **1994**, *17*, 3587–3620. [[CrossRef](#)]
17. Li, Z.; Liu, W.Z.; Zhang, X.C.; Zheng, F.L. Impacts of land use change and climate variability on hydrology in an agricultural catchment on the Loess Plateau of China. *J. Hydrol.* **2009**, *377*, 35–42. [[CrossRef](#)]
18. Fisher, J.B.; Tu, K.P.; Baldocchi, D.D. Global estimates of the land-atmosphere water flux based on monthly AVHRR and ISLSCP-II data, validated at 16 FLUXNET sites. *Remote Sens. Environ.* **2008**, *112*, 901–919. [[CrossRef](#)]
19. Becker, F.; Li, Z.L. Toward a local split window method over land surface. *Int. J. Remote Sens.* **1990**, *11*, 369–393. [[CrossRef](#)]
20. Becker, F.; Li, Z.-L. Surface temperature and emissivity at various scales: Definition, measurement and related problems. *Remote Sens. Rev.* **1995**, *12*, 225–253. [[CrossRef](#)]
21. Sobrino, J.A.; Li, Z.; Stoll, M.P.; Becker, F. Multi-channel and multi-angle algorithms for estimating sea and land surface temperature with ATSR data. *Int. J. Remote Sens.* **1996**, *17*, 2089–2114. [[CrossRef](#)]
22. François, C.; Ottlé, C. Atmospheric corrections in the thermal infrared: Global and water vapor dependent split-window algorithms-applications to ATSR and AVHRR data. *IEEE Trans. Geosci. Remote Sens.* **1996**, *34*, 457–470. [[CrossRef](#)]
23. Sobrino, J.A.; El Kharraz, J.; Li, Z.-L. Surface temperature and water vapour retrieval from MODIS data. *Int. J. Remote Sens.* **2003**, *24*, 5161–5182. [[CrossRef](#)]
24. Becker, F.; Li, Z.L. Temperature-independent spectral indices in TIR bands. *Remote Sens. Environ.* **1990**, *32*, 17–33. [[CrossRef](#)]
25. Li, Z.-L.; Becker, F. Feasibility of land surface temperature and emissivity determination from AVHRR data. *Remote Sens. Environ.* **1993**, *43*, 67–85. [[CrossRef](#)]
26. Valor, E.; Caselles, V. Mapping land surface emissivity from NDVI: Application to European, African, and South American areas. *Remote Sens. Environ.* **1996**, *57*, 167–184. [[CrossRef](#)]
27. Wan, Z.; Li, Z.-L.J. A physics-based algorithm for retrieving land surface emissivity and temperature from EOS/MODIS data. *IEEE Trans. Geosci. Remote Sens.* **1996**, *35*, 980–996.
28. Sobrino, J.A.; Raissouni, N. Toward remote sensing methods for land cover dynamic monitoring: Application to Morocco. *Int. J. Remote Sens.* **2000**, *21*, 353–366. [[CrossRef](#)]
29. Sobrino, J.A.; Raissouni, N.; Li, Z. A Comparative Study of Land Surface Emissivity Retrieval from NOAA Data. *Remote Sens. Environ.* **2001**, *75*, 256–266. [[CrossRef](#)]
30. Li, J.; Li, Z.; Jin, X.; Schmit, T.J.; Zhou, L.; Goldberg, M.D. Land surface emissivity from high temporal resolution geostationary infrared imager radiances: Methodology and simulation studies. *J. Geophys. Res.* **2011**, *116*, 21. [[CrossRef](#)]
31. Li, Z.; Li, J.; Li, Y.; Zhang, Y.; Schmit, T.J.; Zhou, L.; Goldberg, M.D.; Menzel, W.P. Determining diurnal variations of land surface emissivity from geostationary satellites. *J. Geophys. Res.* **2012**, *117*, 33. [[CrossRef](#)]
32. Masiello, G.; Serio, C. Simultaneous physical retrieval of surface emissivity spectrum and atmospheric parameters from infrared atmospheric sounder interferometer spectral radiances. *Appl. Opt.* **2013**, *52*, 2428–2446. [[CrossRef](#)]
33. Masiello, G.; Serio, C.; Venafra, S.; Liuzzi, G.; Götsche, F.; Trigo, I.; Watts, P. Kalman filter physical retrieval of surface emissivity and temperature from SEVIRI infrared channels: A validation and intercomparison study. *Atmos. Meas. Tech.* **2015**, *8*, 2981–2997. [[CrossRef](#)]
34. Sobrino, J.A.; Li, Z.-L.; Stoll, M.P.; Becker, F. Improvements in the split-window technique for land surface temperature determination. *IEEE Trans. Geosci. Remote Sens.* **1994**, *32*, 243–253. [[CrossRef](#)]
35. Price, J.C. Land surface temperature measurements from the split window channels of the NOAA-7/AVHRR. *J. Geophys. Res.* **1984**, *89*, 7231–7237. [[CrossRef](#)]
36. Wan, Z.; Dozier, J. A generalized split-window algorithm for retrieving land-surface temperature measurement from space. *IEEE Trans. Geosci. Remote Sens.* **1996**, *34*, 892–905.
37. JPSS LSTWebsite. Available online: <https://www.star.nesdis.noaa.gov/jpss/> (accessed on 18 September 2023).
38. Berk, A.; Anderson, G.P.; Acharya, P.K.; Chetwynd, J.H.; Bernstein, L.S.; Shettle, E.P.; Matthew, M.W.; Adler-Golden, S.M. *MODTRAN 4 User's Manual*; Air Force Research Laboratory, Space Vehicles Directorate, Air Force Materiel Command: Hascom AFB, MA, USA, 1999.
39. Scott, N.A.; Chedin, A. A fast line by line method for atmospheric absorption computations. *J. Meteorol.* **1981**, *20*, 802–812. [[CrossRef](#)]
40. Hook, S.J. *The ASTER Spectral Library*; Jet Propulsion Lab: Pasadena, CA, USA, 1999. Available online: <http://speclib.jpl.nasa.gov/> (accessed on 13 September 2023).

41. Prata, A.J. Land surface temperatures derived from the AVHRR and the ATSR, 2, Experimental results and validation of AVHRR algorithms. *J. Geophys. Res.* **1994**, *99*, 13025–13058. [[CrossRef](#)]
42. Prata, A.J.; CSIRO Division of Atmospheric Research. Validation Data for Land Surface Temperature Determination from Satellites/A.J. Prata CSIRO Division of Atmospheric Research Aspendale Vic. 1994. Available online: <https://catalogue.nla.gov.au/catalog/695883> (accessed on 18 September 2023).

Disclaimer/Publisher’s Note: The statements, opinions and data contained in all publications are solely those of the individual author(s) and contributor(s) and not of MDPI and/or the editor(s). MDPI and/or the editor(s) disclaim responsibility for any injury to people or property resulting from any ideas, methods, instructions or products referred to in the content.